Molecular Pharmacology Fast Forward. Published on August 12, 2015 as DOI: 10.1124/mol.115.100131
This article has not been copyedited and formatted. The final version may differ from this version.

Identification of a highly conserved allosteric binding site on Mnk1 and Mnk2

Sunita K.C. Basnet, Sarah Diab, Raffaella Schmid, Mingfeng Yu, Yuchao Yang, Todd Alexander Gillam, Theodosia Teo, Peng Li, Tom Peat, Hugo Albrecht and Shudong Wang

Centre for Drug Discovery and Development, Sansom Institute for Health Research, Centre for Drug Discovery and Development, and School of Pharmacy and Medical Sciences, University of South Australia, Adelaide, SA 5001, Australia (S.K.C.B, S.D., R.S., M.Y., Y.Y., T.A.G., T.T., P.L., H.A., S.W).

CSIRO Biosciences Program, 343 Royal Parade, Parkville, Victoria 3052, Australia (T.P.).

Molecular Pharmacology Fast Forward. Published on August 12, 2015 as DOI: 10.1124/mol.115.100131
This article has not been copyedited and formatted. The final version may differ from this version.

Running title page

Running title

Allosteric inhibition of Mnks

Corresponding author

Shudong Wang and Hugo Albrecht

Address: Centre for Drug Discovery and Development, Sansom Institute for Health Research, Centre for Drug Discovery and Development, and School of Pharmacy and Medical Sciences, University of South Australia, Adelaide, SA 5001, Australia

Tel.: +61-8-830 22372; Fax: +61-8-830 21087

E-mail: shudong.wang@unisa.edu.au and Hugo.Albrecht@unisa.edu.au

Number of text pages: 20

Number of tables: 2

Number of schemes: 1

Number of figures: 7

Number of references: 32

Number of words in the Abstract: 225

Number of words in the Introduction: 853

Number of words in the Discussion: 1483

Molecular Pharmacology Fast Forward. Published on August 12, 2015 as DOI: 10.1124/mol.115.100131
This article has not been copyedited and formatted. The final version may differ from this version.

List of non-standard abbreviations

AML, acute myeloid leukemia; BSA, bovine serum albumin; CDK, cyclin-dependent kinase; DTT, dithiothreitol; eIF, eukaryotic initiation factor; ERK, extracellular signal-regulated kinase; FLT3, Fms-like tyrosine kinase 3; GI_{50}, concentration with 50% growth inhibition; GST, glutathione s-transferase; IC_{50}, half maximal inhibitory concentration; IMAP, immobilized metal ion affinity particle; Jak, janus kinase; K_i, inhibition constant; K_m, Michaelis-Menten's constant; MAPK, mitogen-activated protein kinase; Mnk, mitogen activated protein kinase-interacting kinase; mTOR, mammalian target of rapamycin; PI3K, phosphatidylinositol 3-kinase; Pim-1, provirus integration site for Moloney murine leukemia virus-1; PTEN, phosphatase and tensin homolog; Raf, rapidly accelerated fibrosarcoma; Ras, rat sarcoma; Rfu, relative fluorescence units; RLU, relative light units; S/B, signal-to-background ratio; SD, standard deviation; SEM, standard error of mean; TAMRA, tetramethylrhodamine; Tb, terbium; TR-FRET, time resolved fluorescence resonance energy transfer.

Molecular Pharmacology Fast Forward. Published on August 12, 2015 as DOI: 10.1124/mol.115.100131
This article has not been copyedited and formatted. The final version may differ from this version.

Abstract

Elevated levels of phosphorylated eukaryotic initiation factor 4E (eIF4E) have been implicated in many tumor types, and mitogen activated protein kinase (MAPK)-interacting kinases (Mnks) are the only known kinases that phosphorylate eIF4E at Ser209. The phosphorylation of eIF4E is essential for oncogenic transformation, but is of no significance to normal growth and development. Pharmacological inhibition of Mnks therefore provides a non-toxic and effective strategy for cancer therapy. However, a lack of specific Mnk inhibitors has confounded pharmacological target validation and clinical development. Herein, we report the identification of novel series of Mnk inhibitors and their binding modes. A systematic workflow has been established to distinguish between type III and type I/II inhibitors. A selection of 66 compounds was tested for Mnk1 and Mnk2 inhibition and 9 out of 20 active compounds showed type III interaction with an allosteric site of the proteins. Most of the type III inhibitors exhibited dual Mnk1 and Mnk2 activities, and demonstrated potent anti-proliferative properties against the MV4-11 acute myeloid leukemia cell line. Interestingly, ATP-/substrate-competitive inhibitors were found to be highly selective for Mnk2 with little or no activity for Mnk1. Our study suggests that Mnk1 and Mnk2 share a common structure of the allosteric inhibitory binding site, but possess different structural features of the ATP catalytic domain. The findings will assist in the future design and development of Mnk targeted anti-cancer therapeutics.

Molecular Pharmacology Fast Forward. Published on August 12, 2015 as DOI: 10.1124/mol.115.100131
This article has not been copyedited and formatted. The final version may differ from this version.

Introduction

The eukaryotic translation initiation factor 4E (eIF4E) is phosphorylated by mitogen activated protein kinase (MAPK)-interacting kinases (Mnks) and elevated phosphorylation levels are associated with cell proliferation and malignancy. There is growing interest in targeting Mnks as anti-cancer targets (Altman et al, 2013; Diab et al, 2014a; Hou et al, 2012). Specifically, it has been shown in animal models that phosphorylation of eIF4E at Ser209 is crucial for tumor formation (Furic et al, 2010; Ueda et al, 2010) while mice with a Ser209Ala mutation are resistant to tumor development (Furic et al, 2010). Further, mutated and constitutively active Mnk1 is known to drive tumor formation and this corresponds with enhanced eIF4E phosphorylation (Wendel et al, 2007). Finally, $PTEN^{-/-}$ mice crossed with Mnk 1/2 double knockout mice show reduced tumor burden compared to $PTEN^{-/-}$ mice (Ueda et al, 2010). Both Ras/Raf/ERK and PI3K/Akt/mTOR signaling pathways play important roles in oncogenesis, and they are known to synergistically activate the oncogenic eIF4E (Diab et al, 2014a; Hou et al, 2012; Konicek et al, 2011). Therefore, inhibiting eIF4E phosphorylation presents an opportunity to concurrently target two signaling pathways. Several studies have suggested that eIF4E phosphorylation is of no importance for normal cell growth and development (Konicek et al, 2011; Ueda et al, 2004). Despite the fact that Mnks could potentially be effective targets for cancer therapy with better outcomes and fewer side effects, only limited advancement has been made in developing pharmacological inhibitors. For example, CGP57380 has been described as Mnk inhibitor and exhibited activity in cancer cells at micro molar concentrations (Diab et al, 2014b; Teo et al, 2015b; Yu et al, 2015), but it also inhibited several other kinases with similar potency (Bain et al, 2007). Another Mnk inhibitor cercosporamide (Sussman et al, 2004) was recently shown to have

Molecular Pharmacology Fast Forward. Published on August 12, 2015 as DOI: 10.1124/mol.115.100131
This article has not been copyedited and formatted. The final version may differ from this version.

anti-tumor activity in human tumor xenografts (Konicek et al, 2011). However, it also exerted non-specific effects against other kinases. Such off-target effects compromise the pharmacological proof of concept for Mnks as anti-cancer targets.

Kinase inhibitors have been categorized according to distinct mechanisms. Type I inhibitors typically form one to three hydrogen bonds with the hinge region of the kinase (Liu & Gray, 2006), bind to active and inactive conformations (Nagar et al, 2002; Tokarski et al, 2006; Vogtherr et al, 2006; Wodicka et al, 2010), are ATP competitive and often have limited selectivity (Blanc et al, 2013; Zhang et al, 2009), due to interaction with the highly conserved ATP binding pocket. In most cases, type II inhibitors not only form one to three reversible hydrogen bonds at the hinge region of the ATP active site but also interact with the adjacent DFG/D pocket. It has been shown that some type II compounds display stronger binding affinity for kinases when the activation loop adopts the inactive DFG/D-out conformation (Nagar et al, 2002; Tokarski et al, 2006; Vogtherr et al, 2006; Wodicka et al, 2010). Type III inhibitors (colloquially known as allosteric inhibitors) bind exclusively outside of the ATP binding pocket, presumably to non-conserved structural motifs, giving rise to a potentially higher degree of selectivity. These binding modalities are non-ATP-competitive and reversible (Blanc et al, 2013; Eglen & Reisine, 2011).

The aim of the current study was to identify compounds which would potentially be used for the pharmacological validation of Mnks as anti-cancer targets. Our particular interests were (1) discovery of dual and sub-type specific Mnk1/2 inhibitors; (2) identification of type III inhibitors lacking substrate competition with ATP and an eIF4E-derived peptide; and (3) selection of Mnk inhibitors with anti-proliferative effects on leukemia cells. We report the systematic profiling of compounds which were derived from three distinct series. We established a screening cascade which consists of a non-radiometric fluorescence resonance energy transfer (FRET) based immobilized metal ion affinity particle (IMAP) assay for

Molecular Pharmacology Fast Forward. Published on August 12, 2015 as DOI: 10.1124/mol.115.100131
This article has not been copyedited and formatted. The final version may differ from this version.

primary testing, followed by an ADP-Glo assay for dose response and substrate competition analysis. A total of 20 compounds showed inhibitory activities against Mnk2 with IC_{50} < 2 μM. Among of them, 13 compounds were dual inhibitors against Mnk1 and Mnk2 and 7 compounds were sub-type specific, being > 10-fold more potent for Mnk2 over Mnk1. No Mnk1 specific inhibitors were identified. All Mnk inhibitors with IC_{50} values < 2 μM were investigated for substrate competition. In total, 9 inhibitors were found to be non-competitive with both substrates and most of them exerted anti-proliferative activities on MV4-11 acute myeloid leukemia cells. Interestingly, 8 of the non-substrate-competitive compounds were dual inhibitors, suggesting a common allosteric site between Mnk1 and Mnk2.

Molecular Pharmacology Fast Forward. Published on August 12, 2015 as DOI: 10.1124/mol.115.100131
This article has not been copyedited and formatted. The final version may differ from this version.

Materials and Methods

Kinase assays. The IMAP screening kit (Molecular Devices, Sunnyvale, CA) was used for primary Mnk inhibitor screening with a specially designed eIF4E-derived peptide substrate. Hit compound characterization (e.g. IC_{50} determination and substrate competition testing) was conducted with the ADP-Glo kit for ATP concentrations up to 1 mM and the ADP-Glo max kit for higher ATP concentrations up to 6 mM (Promega Corporation, Madison USA).

Peptide substrates. The peptide substrate $eIF4E_{202-214}$ comprised the 13 C-terminal amino acids of human eIF4E (D_{202}TATKSGSTTKNR_{214}). Custom synthesis was carried out by Mimotopes Pty. Ltd. (Victoria, Australia) and this peptide was used with the ADP-Glo assays. The peptide substrate TAMRA-$eIF4E_{202-214}$ was used with the IMAP technology. For this purpose $eIF4E_{202-214}$ was N-terminally linked with tetramethylrhodamine (TAMRA).

Mnk1/2 proteins. Recombinant GST-Mnk1/2 and His-Mnk2 were purchased from Life Technologies and Merck Millipore, respectively.

Compounds. Cercosporamide and CGP57380 (*N*3-(4-fluorophenyl)-1*H*-pyrazolo-[3,4-*d*]pyrimidine-3,4-diamine) were supplied by BioAustralis (Smithfield, NSW, Australia) and Sigma (Castle Hill, NSW, Australia), respectively. These compounds were used as references for kinase assays. Compounds of series 1 (*N*-phenylthieno[2,3-*d*]pyrimidin-4-amines), series 2 (3,4-dimethyl-5-(2-(phenylamino)pyrimidin-4-yl)thiazol-2(3*H*)-ones) and series 3 (*N*-phenyl-1*H*-pyrazolo[3,4-*d*]pyrimidin-3-amine) were synthesized in our laboratory as reported previously (Teo et al, 2015a; Teo et al, 2015b; Yu et al, 2015) (Diab et al, 2014b), and were dissolved in dimethylsulfoxide (DMSO) at 10 mM concentration and stored at -20 °C.

IMAP TR-FRET kinase assay. The kinase reaction was performed in 1× IMAP reaction buffer with Tween-20, dithiothreitol (DTT) and distilled H_2O according to manufacturer's protocol using the TAMRA-$eIF4E_{202-214}$ peptide substrate. The test compounds were added to

Molecular Pharmacology Fast Forward. Published on August 12, 2015 as DOI: 10.1124/mol.115.100131
This article has not been copyedited and formatted. The final version may differ from this version.

the above kinase reaction mixture at 1 and 10 µM final concentrations with DMSO content of 0.5%. Then each Mnk kinase was diluted with 1× IMAP reaction buffer containing Tween-20 (see manufacturer's protocol) and added to the reaction mixture. The kinase reaction was started by final addition of ATP and incubated at 30° C for 90 min in a total assay volume of 20 µL. The reaction was stopped by adding 60 µL of progressive binding solution (30% binding buffer A, 70% binding buffer B, progressive binding reagent 1:600 and terbium (Tb)-donor (1:400) and the plate was then read in an EnVision Multilabel plate reader (PerkinElmer, Buckinghamshire, UK) following 5 hours of incubation in the dark. The excitation wavelength for the Tb-donor was set at 330 nm and the emissions of the Tb-donor and the TAMRA-eIF4E$_{202-214}$ substrate (TR-FRET signal) were recorded at 545 and 572 nm, respectively. The emission was measured in a time resolved mode with a delay of 200 µsec. Positive and negative controls were carried out in 0.5% DMSO in presence and absence of Mnk kinases, respectively. For dose response experiments with control Mnk inhibitors (CGP57380 and cercosporamide), the kinase reaction was run in a similar way with an inhibitor dilution factor of 1:3 for 8 concentrations ranging from 10 µM to 4.5 nM in 0.5% DMSO.

ADP-Glo kinase assay. Assay kits from Promega Corporation were used according to instructions and adapted as outlined in the results section. Test compounds were generally prepared with 1:3 serial dilutions for 8 concentrations (from 10 µM to 4.5 nM); 10 concentrations were used (15 µM to 0.7 nM) for substrate competition experiments. The kinase reaction was performed with 1× kinase reaction buffer (40 nM Tris base pH 7.5, 20 mM $MgCl_2$, 0.4 mM DTT), 0.1 mg/ml BSA, distilled H_2O, eIF4E$_{202-214}$ substrate and Mnk kinases in a total assay volume of 15 µL following the manufacturer's protocol. In brief: The kinase reactions were started by addition of ATP, incubated for 45 min at 30° C and then stopped by adding 15 µL of ADP Glo reagent. After incubation at room temperature in the

Molecular Pharmacology Fast Forward. Published on August 12, 2015 as DOI: 10.1124/mol.115.100131
This article has not been copyedited and formatted. The final version may differ from this version.

dark for 40 min, 30 µL of kinase detection reagent was added per well and incubated for 30-60 min depending on the ATP concentration used in the kinase reaction (10-100 µM: 30 min, 100-500 µM: 40 min, 500-1000 µM: 60 min). For higher concentrations of ATP (up to 6 mM), the ADP-Glo max kit was used which is similar to ADP-Glo kinase assay but adapted for high ATP concentrations as used in ATP competition experiments. The incubation time after addition of the detection reagent was 60 min for this assay. Luminescence was measured using an EnVision multilabel plate reader (PerkinElmer, Buckinghamshire, UK) with an integration time of 1 sec per well. Positive and negative controls were performed in 0.5% DMSO in presence and absence of Mnk kinases, respectively. Standard curves with defined ADP/ATP ratios were routinely performed and used to convert relative light units (RLU) into reaction velocities (e.g. V_{max} calculation).

Data analysis. Microsoft Excel or Graphpad Prism software (version 6.0) was used for data analysis.

The normalized TR-FRET signal was calculated by dividing the relative fluorescence units (Rfu) measured from the TR-FRET emission (572 nm) by the Tb emission (545 nm) and multiplied by 10'000:

$$TR\text{-}FRET = \frac{TR\text{-}FRET\ Rfu}{Tb\ Rfu} * 10'000$$

Determination of the maximal velocity (V_{max}) and Michaelis-Menten constant (K_m) were carried out using Michaelis-Menten curve fitting.

Dose response curves (IC_{50} and GI_{50}) were calculated using a 4-parameter logistic non-linear regression model.

Molecular Pharmacology Fast Forward. Published on August 12, 2015 as DOI: 10.1124/mol.115.100131
This article has not been copyedited and formatted. The final version may differ from this version.

The Z'-factor (Zhang et al, 1999) was routinely calculated to quantify the assay performance according to the following equation:

$$Z' = 1 - \frac{3 * (\sigma_p + \sigma_n)}{(\mu_p - \mu_n)}$$

Where σ_p = Standard deviation (SD) of positive controls; σ_n = SD of negative controls; μ_p = mean of positive controls; μ_n = mean of negative controls.

The Pearson Correlation was calculated with the following formula:

$$Correl(X,Y) = \frac{\sum(x-\overline{x})(y-\overline{y})}{\sqrt{\sum(x-\overline{x})^2 \sum(y-\overline{y})^2}}$$

Where x were the IC_{50} values and y were the GI_{50} values.

Kinase profiling. Inhibition of CDK2 and CDK9 were measured using a radiometric assay by Eurofins Pharma Discovery Services UK Limited using ATP concentration within 15 μM of K_m for each kinase. The half maximal inhibitory concentration (IC_{50}) values were determined from 10 data point dose response experiments, and the inhibitory constants (K_i) were calculated from IC_{50} values and K_m (ATP) values for each kinase.

Cell culture. MV4-11 cells were kindly provided by Prof. Richard D'Andrea (University of South Australia) and maintained in Roswell Park Memorial Institute medium (RPMI)-1640 with 10% fetal bovine serum (FBS).

Proliferation assay. Resazurin (Sigma) assay was carried out in MV4-11 cells as previously reported (Diab et al, 2014b). The compound concentration required to inhibit cell proliferation by 50 % (GI_{50}) was calculated using non-linear regression analysis.

Molecular Pharmacology Fast Forward. Published on August 12, 2015 as DOI: 10.1124/mol.115.100131
This article has not been copyedited and formatted. The final version may differ from this version.

Western blotting. MV4-11 cells were seeded at 8×10^5 cells/10 mL of medium. After 24 hours cells were treated with 8 different concentrations of inhibitors for 1h. Protein concentration was determined by DC assay (Bio-Rad) and a total of 20 µg protein was separated by SDS-PAGE and transferred onto nitrocellulose membranes. Primary antibodies against Ser209 phosphorylated eIF4 (p-eIF4E^{Ser209}), eIF4E or β-actin were used (Cell Signaling Technologies, Danvers, MA). A secondary anti-rabbit immunoglobulin G (IgG) horseradishperoxidase (HRP)-conjugated antibody was used (Dako, Glostrap, Denmark) to develop the western blot with Enhanced Chemiluminescence (ECL) reagents (GE Life Sciences). IC_{50} values were determined by applying a 4-parameter logistic non-linear regression model.

Results

Identification of dual Mnk1/2 and mono-specific Mnk2 inhibitors. The initial step to establish the compound profiling workflow as outlined in Scheme 1 required to develop non-radioactive kinase assays based on the IMAP technology. To achieve this, a 13 amino acid peptide i.e. DTATKSGS$_{209}$TTKNR (eIF4E$_{202-214}$), which contains the Mnk1/2 phosphorylating residue Ser209 and is a fragment based on the C-terminal sequence of human eIF4E, was custom synthesized. The peptide was N-terminally linked to the fluorescent FRET acceptor TAMRA leading to the IMAP kinase substrate TAMRA-eIF4E$_{202-214}$ (Figure 1A). The fluorescently labeled peptide is phosphorylated by the Mnks and the IMAP binding reagent stops the kinase reaction and binds the phosphorylated substrate through high affinity interaction of trivalent metal-containing (M^{III}) nanoparticles. The phosphorylated and bound substrate can be detected by TR-FRET between the Tb-donor and the TAMRA acceptor on the peptide. Optimization of assay conditions started with

Molecular Pharmacology Fast Forward. Published on August 12, 2015 as DOI: 10.1124/mol.115.100131
This article has not been copyedited and formatted. The final version may differ from this version.

incubation of the peptide substrate TAMRA-eIF4E$_{202-214}$ at 5 µM with different amounts of Mnk1 or Mnk2 in a standard kinase reaction using 100 µM ATP (Figure 1B). To obtain a sufficient signal-to-background ratio (S/B) and to minimize enzyme consumption, 100 ng of Mnk1 (S/B = 2.3) and 50 ng of Mnk2 (S/B = 2.5) were used in all subsequent experiments. The second step for optimization was to test the TAMRA-eIF4E$_{202-214}$ substrate at three concentrations, and sufficient S/B ratios were detected at 5 µM (S/B = 2.4 for Mnk1 and S/B = 2.6 for Mnk2) (Figure 1C). Assay conditions were further optimized by testing ATP at various concentrations in the presence of Mnk 1 or Mnk2, and increasing signals were detected with both kinases to approximately 200 µM ATP, followed by a rapid decrease of the signal (Figure 1D). The first five data points were used to determine suitable ATP concentrations for the primary compound profiling. Iterative fitting to the Michaelis-Menten model was carried out with the Prism software and we estimated that half maximal signals will be reached at 165 and 80 µM for Mnk1 and Mnk2, respectively. These ATP concentrations were applied to perform dose response experiments with two known inhibitor compounds CGP57380 and cercosporamide using 100 ng of Mnk1 or 50 ng of Mnk2 and 5 µM TAMRA-peptide substrate. CGP57380 and cercosporamide showed an IC_{50} value of 1.51 and 0.67 µM with Mnk1. The corresponding values for Mnk2 were 1.87 and 0.16 µM (Figure 1E).

A collection of 66 compounds was generated for pharmacological target validation of Mnk1 and Mnk2. 29 compounds (series 1, Supplemental Table 1) were derived from patented *N*-phenylthieno[2,3-*d*]pyrimidin-4-amines (WO2010/023181) (Teo et al, 2015a; Teo et al, 2015b), 31 compounds (series 2, Supplemental Table 1) were developed based on our privileged structures of 5-(2-(phenylamino)pyrimidin-4-yl)thiazol-2(3*H*)-one (Diab et al, 2014b) and 6 compounds were the derivatives of *N*-phenyl-1*H*-pyrazolo[3,4-*d*]pyrimidin-3-amine (series 3, Supplemental Table 1). All compounds were tested with the IMAP assays at

Molecular Pharmacology Fast Forward. Published on August 12, 2015 as DOI: 10.1124/mol.115.100131
This article has not been copyedited and formatted. The final version may differ from this version.

two concentrations (1 µM and 10 µM) in duplicate and the averages of relative activities were calculated for both concentrations (Figure 2A and 2B). Allover, 31 compounds caused a reduction of Mnk1 and/or Mnk2 kinase activity to less than 75% at 1 µM or 10% at 10 µM. Under these criteria, 18 actives were considered as Mnk2 specific, 11 were dual inhibitors and only 2 were identified as Mnk1 specific (Scheme 1); the latter showed only weak efficacy with residual activities > 65% and > 70% at 10 µM and 1 µM, respectively. Assay robustness was routinely checked by monitoring the correlation of duplicate data points (Figures 2C and 2D) and by calculating Z'-factors from four positive and negative controls which were included in all experiments (Figure 2E). The calculated Z'-factors were all larger than 0.5, which indicated both assays to be sufficiently robust.

Mnk1 and Mnk2 show different kinetic properties and ligand-binding profiles. The IMAP assays can be run at relatively low cost and are very robust; however they are not suitable for kinetic characterization of the interactions between kinases and ligands. This is due to the limited compatibility with ATP concentrations (Figure 1D). Therefore, we established the ADP-Glo assay which measures ATP depletion during the kinase reaction (Figure 3A). With this assay format the kinase reaction is conducted with Mnk and $eIF4E_{202-214}$ peptide and stopped after the optimized incubation time. Addition of the ADP-Glo reagent stops the reaction and drives the enzymatic removal of the leftover ATP. In the next step the kinase detection reagent is used to enzymatically convert ADP back into ATP which then is utilized to drive a luciferase reaction. The luminescence signal is directly proportional to the amount of ADP generated during the kinase reaction. The assays can generally be used with ATP concentrations up to 6 mM, and therefore are suitable for determination of K_m and V_{max} values. Besides, the assays are appropriate to distinguish between ATP competitive and non-ATP-competitive inhibitors by varying concentrations of ATP in the kinase reaction. In the first step of the assay development, we explored suitable Mnk concentrations. Various

Molecular Pharmacology Fast Forward. Published on August 12, 2015 as DOI: 10.1124/mol.115.100131
This article has not been copyedited and formatted. The final version may differ from this version.

amounts of activated recombinant Mnk1 or Mnk2 were incubated with 100 µM ATP and 100 µM eIF4E$_{202-214}$ substrate. The kinase reactions were performed without the substrate as controls. Sufficiently robust signals were achieved with 100 ng Mnk1 and 30 ng Mnk2, which resulted in S/B ratios of 6.2 and 3.4, respectively (Figure 3B). These amounts of enzyme were applied for all further experiments. In the next step K_m and V_{max} values were determined for the eIF4E$_{202-214}$ substrate (Table 1). For this purpose, the ATP concentration was fixed at 2 mM and tested against eIF4E$_{202-214}$ substrate at a range of concentrations (Figure 3C). Michaelis-Menten curve fit with baseline corrected data (obtained from the kinase reaction without eIF4E$_{202-214}$), revealed a K_m value of 1.272 mM and the determined V_{max} value was used to calculate the maximal specific activity (eIF4E-derived peptide turn over per minute) of 2172 nmol/min/mg for Mnk1. The respective values for Mnk2 were 608.5 µM for K_m and 1846 nmol/min/mg for the specific activity. Subsequently we determined K_m and V_{max} values for ATP using 100 ng Mnk1 or 30 ng Mnk2 with the eIF4E-derived peptide substrate at a fixed concentration of 1.2 mM (Figure 3D). Control reactions were run without kinase and used for background correction. Michaelis-Menten curve fit resulted in a K_m value of 2.094 mM and a specific activity of 1852 nmol/min/mg for Mnk1 under V_{max} conditions. The corresponding values for Mnk2 were significantly lower with 215.8 µM for K_m and 1075 nmol/min/mg for the specific activity (Table 1). Dose response testing with enzyme inhibitors is often carried out using substrate concentrations which correspond to the K_m value. Mnk1 showed very high K_m values for ATP and the peptide substrate, therefore we reduced ATP and peptide concentrations correspondent to 50% of the K_m values in order to cut consumable costs. The S/B ratio under these conditions was 14.2 and seemed sufficient for dose response experiments (data not shown). For all further tests the ATP and peptide concentrations were adjusted to 50% of the K_m values for Mnk1 and K_m values were used for Mnk2. Finally, we investigated the dose response of the control

Molecular Pharmacology Fast Forward. Published on August 12, 2015 as DOI: 10.1124/mol.115.100131
This article has not been copyedited and formatted. The final version may differ from this version.

inhibitors CGP57380 and cercosporamide with the optimized ADP-Glo assay on both Mnks by using the aforementioned parameters in a final assay volume of 15 µL. IC_{50} values were calculated by applying a 4-parameter logistic non-linear regression model. CGP57380 and cercosporamide showed K_i values on Mnk1 of 1.01 µM and 0.507 µM, respectively. The corresponding values on Mnk2 were 0.877 µM and 0.079 µM, respectively (Figure 3E and Table 1).

All compounds causing residual kinase activities of < 75% at 1 µM and/or of < 10 % at 10 µM as determined in the primary IMAP assay (Figure 2A and 2B) were selected as hits and were subjected to further analysis of enzyme kinetics using the ADP-Glo kinase assay. Dose response experiments were performed to determine IC_{50} values (Table 2). At this stage, particular emphasis was put on the identification of dual and Mnk sub-type specific inhibitors. Seven compounds (MNKI-4, -12, -28, -67, -85, -4-61 and -5-17) were identified as Mnk2 specific inhibitors with IC_{50} values being at least 10 times lower for Mnk2 than for Mnk1; 13 compounds (MNKI-5, -6, -7, -8, -15, -19, -37, -57, -83, -2-22, -2-25, -2-30 and -7-50) were considered as dual inhibitors whilst no Mnk1 specific inhibitors were identified (Figure 3F and Scheme 1).

Identification of dual Mnk1/2 inhibitors with Type III mechanism. The main objective of this work was to select specific chemical probes which would be useful for the future pharmacological validation of Mnks as anti-cancer drug targets. To achieve this, it is imperative to identify compounds with high specificity. Type III inhibitors are believed to have a tendency to achieve higher specificity due to the fact that the strongly conserved ATP binding pocket is not involved in the binding modalities. To achieve our goal, a total of 20 actives were investigated using the ADP-Glo assay for competing effects at elevated ATP concentrations. All compounds were tested at 10 concentrations ranging from 0.7 nM to 15 µM with 100 ng Mnk1 using 150, 2000 or 6000 µM ATP. In parallel the same dose range was

Molecular Pharmacology Fast Forward. Published on August 12, 2015 as DOI: 10.1124/mol.115.100131
This article has not been copyedited and formatted. The final version may differ from this version.

tested with 30 ng Mnk2 using 50, 200 or 2000 μM ATP. The eIF4E$_{202-214}$ peptide substrate concentrations were fixed for Mnk1 and Mnk2 at 1.2 mM and 0.6 mM, respectively. The IC_{50} values were systematically calculated for all conditions and the ratios between the highest and lowest ATP concentrations are given in Table 2 (IC_{50} ratio). Subsequently, a similar set of experiments were conducted to investigate competition effects of elevated eIF4E$_{202-214}$ concentrations. The peptide substrate was tested at 150, 600 and 3000 μM with ATP fixed at 2 mM for Mnk1 and 200 μM for Mnk2. The IC_{50} values were routinely calculated and competing effects were assessed by the ratios obtained at the highest substrate concentration versus the one at the lowest substrate concentration (Table 2). We arbitrarily set a ratio > 5 as a significant competing effect. With this criterion, we proposed different inhibitory mechanisms as outlined below:

Non-substrate- and non-ATP-competitive inhibitors (mode -/-): These compounds did not show significant change in the IC_{50} values when ATP or the eIF4E$_{202-214}$ substrate were used at increased concentrations. Compounds with this type of inhibitory properties are depicted with mode -/- in Table 2.

ATP-competitive inhibitors (mode +/-): These compounds showed significant increase in the IC_{50} values at elevated ATP concentrations but showed no or at the most marginally changed IC_{50} values with increased eIF4E$_{202-214}$ concentrations.

Dual substrate- and ATP-competitive inhibitors (mode +/+): IC_{50} values were affected by increased ATP and peptide substrate levels. Only one compound (MNKI-5-17) showed this property and was only active against Mnk2.

Substrate-competitive inhibitors (mode -/+): Only one compound (MNKI-2-22) showed a moderate competitive effect with eIF4E$_{202-214}$ peptide on Mnk2 (Table 2). Surprisingly, when

Molecular Pharmacology Fast Forward. Published on August 12, 2015 as DOI: 10.1124/mol.115.100131
This article has not been copyedited and formatted. The final version may differ from this version.

tested on Mnk1, the same compound showed a moderate competition effect with ATP but no effect with eIF4E$_{202-214}$.

A selection of compounds was re-tested with the same conditions as outlined above, using an extended range of ATP concentrations (Figure 4A-C) whilst the eIF4E$_{202-214}$ substrate concentrations were fixed at K_m. Data from individual dose response curves were analyzed using Prism 6 Graphpad software and plotted as a function of log transformed inhibitor concentration. The representative examples are shown in Figures 4A-C. A similar set of experiments was carried out to evaluate effects of the eIF4E$_{202-214}$ peptide, the ATP concentrations were fixed at K_m value (Figure 4D-F).

The data were further used to calculate apparent K_m and V_{max} values at various concentrations of inhibitors. A representative example for mode -/- on Mnk2 is given in Figure 5A and D. Increasing compound concentrations led to lower V_{max} values for ATP and eIF4E$_{202-214}$ while the K_m values remained unchanged, as it would be expected for a type III non-competitive inhibitory mechanism. Additional examples are given for modes +/- and +/+ in Figure 5B/E and 5C/F, respectively. Mode +/- showed increased K_m values for ATP combined with unchanged V_{max} values, which is an expected characteristic of competitive enzyme inhibition (Gumireddy et al, 2005). Finally, for mode +/+ elevated K_m values were calculated with increased ATP and eIF4E$_{202-214}$ concentrations. No major changes of the V_{max} values were observed.

Cytotoxic effects on MV4-11 acute leukemia cells. Anti-proliferative activity of the inhibitors was evaluated in MV4-11 cells using the resazurin assay. Cells were exposed to each compound for 72 h, and the values of concentration that causes 50% growth inhibition (GI_{50}) were summarized in Table 2. All compounds with a GI_{50} value < 15 μM were further tested for inhibitory activity against CDK2A and CDK9T1; if the resulting residual kinase

Molecular Pharmacology Fast Forward. Published on August 12, 2015 as DOI: 10.1124/mol.115.100131
This article has not been copyedited and formatted. The final version may differ from this version.

activities were < 60% at 10 μM, a K_i value determination was carried out. Finally, all compounds with K_i values < 15 μM for either CDK were excluded from further analysis (Table 2). The remaining 17 compounds were analyzed for the correlation between IC_{50} values on Mnks and GI_{50} values on MV4-11 cells (Figure 6). Mnk1 inhibitors with an IC_{50} value > 10 μM were excluded, resulting in a total of 14 compounds. The discrepancy between biochemical and cellular potencies are expected as cellular activity may be influenced by physicochemical properties of compounds which may affect permeability across the cell membrane, intra-cellular degradation and so forth. Nevertheless a clear correlation was observed for both Mnk1 and Mnk2 inhibitors. The Pearson correlation was calculated to 0.4006 and 0.7276 for Mnk1 and Mnk2, respectively. The corresponding one tailed p values were 0.078 and 0.0005. The cellular Mnk inhibition was further confirmed with western blotting analysis of MV4-11 cells after treatment with two Mnk inhibitors i.e. MNKI-7 or MNKI-19 for one hour. A dose-dependent down-regulation of phosphorylation at Ser209 of eIF4E was detected (Figures 6C and 6D).

Discussion

To identify Mnk inhibitors we established a screening cascade (Scheme 1). The IMAP Mnk1/2 assays enabled us to rapidly identify primary hits while the ADP-Glo assay facilitated the dose-response analysis. The sequential use of these mechanistically different assay technologies (identification of phosphorylated peptide vs. ATP depletion) excluded any false positives.

For the IMAP assay, we successfully used a TAMRA-labeled eIF4E-derived peptide ($eIF4E_{202-214}$) to detect kinase activities of Mnk1 and Mnk2 in the presence of tested compounds. However the assay was incompatible with high ATP concentrations above 200

μM (Figure 1D). This effect was most likely due to the displacement of the phosphorylated substrate from the IMAP nano-beads by ATP phosphate groups, leading to a reduced FRET signal. This inherent property of the IMAP assay limits it's suitability for experiments requiring high ATP concentrations (e.g. ATP competition testing). However, at relatively low ATP concentrations the assay was shown to be very robust and cost effective for initial compound profiling. Finally, the IMAP assays were validated with the known Mnk inhibitors CGP57380 and cercosporamide (Figure 1E), and the obtained inhibitory activity against Mnk1/2 were consistent with the published data (Bain et al, 2007; Buxade et al, 2005; Konicek et al, 2011). One advantage of using low ATP concentrations in the assays was to identify weak ATP-competitive and type II inhibitors which would be lost at higher ATP concentrations.

Three different chemical series of compounds were profiled at the concentrations of 1 and 10 μM by IMAP assays. Figures 2A and 2B show the averages of the measured residual kinase activities for Mnk1 and Mnk2, respectively. Figures 2C and 2D are scatter plots of duplicate data points with a trend line. The calculated R^2 correlations of 0.897 and 0.879 indicated sufficient robustness of the assays and this was further confirmed by the routinely calculated Z'-factors which were always > 0.5. From the total of 31 primary hits only 2 were Mnk1 specific, 11 were dual inhibitors and 18 were Mnk2 specific.

In contrast to the IMAP assay, the ADP-Glo assay can be run at much higher ATP concentrations and thus is suited to determine kinetic parameters such as K_m and V_{max} values. We established the ADP-Glo assay for Mnk1 and Mnk2 as outlined in Figure 3. Surprisingly, the K_m value for ATP was at 2.094 mM for Mnk1 almost 10 times higher than for Mnk2 (Figure 3D and Table 1). This strongly indicated a lower affinity of ATP for Mnk1 than Mnk2 which is most likely due to structural differences between Mnk1 and Mnk2. The longer C-terminus of Mnk1 is known to affect its basal kinase activity and to repress

Molecular Pharmacology Fast Forward. Published on August 12, 2015 as DOI: 10.1124/mol.115.100131
This article has not been copyedited and formatted. The final version may differ from this version.

phosphorylation of the activation loop (Goto et al, 2009; Parra et al, 2005). Dose response curves with kinase inhibitors are routinely run with the substrate concentrations adjusted to K_m. Due to the fact that K_m values were very high for Mnk1, we decided to reduce the substrate concentrations to 50% of the K_m values for ATP and the peptide substrate. For Mnk2 the concentrations were adjusted to K_m. The K_i values for CGP57380 and cercosporamide (Figure 3E and Table 1) were determined as a final validation step and the obtained results were comparable to literature values (Bain et al, 2007; Buxade et al, 2005; Konicek et al, 2011).

All compounds causing residual kinase activities of < 75% at 1 µM or of < 10% at 10 µM in the IMAP assay (Figure 2A and 2B) were subjected to systematic determination of IC_{50} values with the ADP-Glo assay. In total, 20 inhibitors were identified with IC_{50} values of < 2 µM. Seven inhibitors were Mnk2 specific with a ratio of IC_{50Mnk1}/IC_{50Mnk2} > 10 and 13 inhibitors were dual inhibitors (Figure 3F and Table 2). Out of the 20 compounds 17 belonged to series 1, whilst only 2 and 1were from series 2 and 3, respectively. Interestingly, we did not identify any Mnk1 sub-type specific inhibitors, further indicating significant structural differences between Mnk1 and Mnk2. Analysis of crystal structures of the Mnk1 and Mnk2 kinase domains (Jauch et al, 2006; Jauch et al, 2005) suggests that Mnk2 has a larger ATP binding pocket than Mnk1. Our Mnk2 specific inhibitors provide a new opportunity to dissect biological functions of Mnk1 and Mnk2. It is currently not known whether the individual or combined inhibition of Mnk1/2 would be efficacious in induction of cancer cell apoptosis.

It has generally believed that non-ATP-competitive ligands may provide a selectivity advantage over their ATP-competitive counterparts. We tested our compounds for ATP- and/or $eIF4E_{202-214}$ competition before investigating their toxicity on cancer cell lines. IC_{50} ratios of dose response experiments at high and low ATP or $eIF4E_{202-214}$ concentrations are

Molecular Pharmacology Fast Forward. Published on August 12, 2015 as DOI: 10.1124/mol.115.100131
This article has not been copyedited and formatted. The final version may differ from this version.

given in Table 2. We identified 2 distinct groups: 9 compounds did not show any competition with either of the substrates (mode -/-) and 9 compounds were only competitive with ATP (mode +/-). In addition, 2 compounds were competitive with ATP and $eIF4E_{202-214}$ (mode +/+). Interestingly, MNKI-2-22 showed the inhibitory activities in an ATP competitive manner in Mnk1, but being substrate dependent in Mnk2 (Scheme 1 & Table 2). All compounds with mode -/- belonged to series 1, showed IC_{50} values < 1.6 μM and were associated with dual inhibition of Mnk1 and Mnk2 (except MNKI-67). These findings indicate that these inhibitors act via an allosteric type III mechanism, and we thus conclude that an allosteric binding site is structurally conserved between Mnk1 and Mnk2. In contrast, all compounds with mode +/- had IC_{50} values > 2.8 μM on Mnk1 and 6 of them were Mnk2 specific. Most intriguingly, very subtle structural changes resulted in switched activity modes. For example, MNKI-4-61 of series 2 turned from mode +/- to mode +/+ when 2,4-dimethoxyaniline was replaced with 2-(difluoromethoxy)aniline of MNKI-5-17 (Figure 4). In the case of MNKI-5, the removal of the 1,3-difluoropropan-2-ol group resulted in a change from mode -/- to mode +/- of MNKI-15 and the potency against Mnk1 was reduced by almost factor of 20 (Figure 7A, Table 2). In contrast, when only the fluorides were removed from the 1,3-difluoropropan-2-ol group (MNKI-37) the mode -/- was maintained but reduction of Mnk1 activity by almost 10 fold was observed. Clearly the 1,3-difluoropropan-2-ol group prevents competition with ATP. Finally, when the acetamide on the dihydrothiophene ring of MNKI-37 was replaced with N-(3-methoxypropyl) acetamide (MNKI-83), Mnk1 inhibitory activity was enhanced. There is currently no structural data available for activated Mnk1 (Kumarasiri et al, 2015) and these inhibitory modes remain to be elucidated. The very subtle structural changes resulting in the different inhibitory modes led us to believe that the binding site on the kinases is very close to the targeting sites of ATP and the peptide substrate. We propose the hypothetical models as shown in Figure 7B. The inactive DFD-out conformation

Molecular Pharmacology Fast Forward. Published on August 12, 2015 as DOI: 10.1124/mol.115.100131
This article has not been copyedited and formatted. The final version may differ from this version.

(I) switches into the active DFD-in (II) through phosphorylation of the activation segment by ERK1/2 or p38 kinases. The activated kinase coordinates the ATP and the peptide substrate (eIF4E) in contact with catalytically important residues on the activation segment, the glycine rich loop and the catalytic loop. MNKI-5 is allosteric but shares the same core scaffold (indicated as black diamond in diagram III and IV) with MNKI-15. The latter may have significant binding affinities adjacent to and inside of the ATP binding pocket so to exhibit its Type II mechanism (Figure 7B/III). The loss of ATP competition of MNKI-5 may be caused by its 1,3-difluoropropan-2-ol mediated conformational changes so that it moves away from interacting with the ATP binding site (Figure 7B/IV).

We have previously shown that inhibition of Mnks caused cell-type specific cytoxicity (Diab et al, 2014b; Yu et al, 2015). Most pronounced cytotoxic effects have been observed in FLT3 over-expressing leukemia cells (Altman et al, 2013; Diab et al, 2014b; Lim et al, 2013; Teo et al, 2015a). Accordingly the cytotoxic assay in MV4-11 cells was included in the screening cascade. To determine whether Mnk inhibition was responsible for the observed cytotoxic effects and to assess potential and off-target effects, we first carried out additional kinase testing against CDK2A and CDK9T1 as some derivatives of the chemical series have been shown to be CDK2/9 modulators (Diab et al, 2014b; Shao et al, 2013). Three compounds were excluded from further analysis due to activities on CDKs. The study with the remaining inhibitors showed positive correlations (Pearson correlation $r = 0.4006$ and $r = 0.7276$ for Mnk1 and Mnk2, respectively) between Mnk inhibitory activity and cytotoxic effects, confirming the Mnk specific activity of the compounds. Our western blot analysis also demonstrated a dose-dependent reduction in eIF4E phosphorylation after 1 hour exposure to MNKI-7 or MNKI-19 (Figures 6C and 6D).

Taken together, our investigation suggests significant structural differences in the ATP catalytic domain between Mnk1 and Mnk2 leading to very different inhibitory activities with

Molecular Pharmacology Fast Forward. Published on August 12, 2015 as DOI: 10.1124/mol.115.100131
This article has not been copyedited and formatted. The final version may differ from this version.

ATP-competitive inhibitors. However, both enzymes share a common structural feature of the allosteric binding site that is located in close proximity of the ATP and peptide substrate targeting sites. These findings will be invaluable for the future design, optimization and development of highly specific Mnk inhibitors as therapeutic agents.

Authorship Contributions

Research design: Wang, Albrecht, Basnet, Schmid.

Conducted experiments: Basnet, Schmid, Diab, Yu, Yang, Gillam, Teo, Li.

Performed data analysis: Albrecht, Basnet, Wang.

Wrote or contributed to the writing of the manuscript: Albrecht, Basnet, Yu, Diab, Teo, Peat, Wang.

References

Altman JK, Szilard A, Konicek BW, Iversen PW, Kroczynska B, Glaser H, Sassano A, Vakana E, Graff JR, Platanias LC (2013) Inhibition of Mnk kinase activity by cercosporamide and suppressive effects on acute myeloid leukemia precursors. *Blood* **121:** 3675-3681.

Bain J, Plater L, Elliott M, Shpiro N, Hastie CJ, Mclauchlan H, Klevernic I, Arthur JSC, Alessi DR, Cohen P (2007) The selectivity of protein kinase inhibitors: a further update. *Biochem J* **408:** 297-315.

Blanc J, Geney R, Menet C (2013) Type II kinase inhibitors: an opportunity in cancer for rational design. *Anticancer Agents Med Chem* **13:** 731-747.

Buxade M, Parra JL, Rousseau S, Shpiro N, Marquez R, Morrice N, Bain J, Espel E, Proud CG (2005) The Mnks are novel components in the control of TNFα biosynthesis and phosphorylate and regulate hnRNP A1. *Immunity* **23:** 177-189.

Diab S, Kumarasiri M, Yu M, Teo T, Milne R, Proud C, Wang S (2014a) MAP Kinase-interacting kinases — the emerging targets against cancer. *Chem Biol* **21:** 441–452.

Diab S, Teo T, Kumarasiri M, Li P, Yu M, Lam F, K. C. Basnet S, Sykes MJ, Albrecht H, Milne R et al. (2014b) Discovery of 5-(2-(Phenylamino) pyrimidin-4-yl) thiazol-2 (3H)-one Derivatives as Potent Mnk2 Inhibitors: Synthesis, SAR Analysis and Biological Evaluation. *Chemmedchem* **9:** 962–972.

Eglen R, Reisine T (2011) Drug discovery and the human kinome: recent trends. *Pharmacol Ther* **130:** 144-156.

Furic L, Rong L, Larsson O, Koumakpayi IH, Yoshida K, Brueschke A, Petroulakis E, Robichaud N, Pollak M, Gaboury LA et al. (2010) eIF4E phosphorylation promotes tumorigenesis and is associated with prostate cancer progression. *Proc Natl Acad Sci U S A* **107:** 14134-14139.

Goto S, Yao Z, Proud C (2009) The C-terminal domain of Mnk1a plays a dual role in tightly regulating its activity. *Biochem J* **423:** 279-290.

Gumireddy K, Reddy MR, Cosenza SC, Nathan RB, Baker SJ, Papathi N, Jiang J, Holland J, Reddy EP (2005) ON01910, a non-ATP-competitive small molecule inhibitor of Plk1, is a potent anticancer agent. *Cancer Cell* **7:** 275-286.

Hou J, Lam F, Proud C, Wang S (2012) Targeting Mnks for cancer therapy. *Oncotarget* **3:** 118-131.

Jauch R, Cho MK, Jäkel S, Netter C, Schreiter K, Aicher B, Zweckstetter M, Jäckle H, Wahl MC (2006) Mitogen-activated protein kinases interacting kinases are autoinhibited by a reprogrammed activation segment. *EMBO J* **25:** 4020-4032.

Jauch R, Jäkel S, Netter C, Schreiter K, Aicher B, Jäckle H, Wahl MC (2005) Crystal structures of the Mnk2 kinase domain reveal an inhibitory conformation and a zinc binding site. *Structure* **13:** 1559-1568.

Konicek BW, Stephens JR, McNulty AM, Robichaud N, Peery RB, Dumstorf CA, Dowless MS, Iversen PW, Parsons S, Ellis KE et al. (2011) Therapeutic inhibition of MAP kinase interacting kinase blocks eukaryotic initiation factor 4E phosphorylation and suppresses outgrowth of experimental lung metastases. *Cancer Res* **71:** 1849-1857.

Kumarasiri M, Teo T, Wang S (2015) Dynamical insights of Mnk2 kinase activation by phosphorylation to facilitate inhibitor discovery. *Future Med Chem* **7:** 91-102.

Lim S, Saw TY, Zhang M, Janes MR, Nacro K, Hill J, Lim AQ, Chang CT, Fruman DA, Rizzieri DA et al. (2013) Targeting of the MNK–eIF4E axis in blast crisis chronic myeloid leukemia inhibits leukemia stem cell function. *Proc Natl Acad Sci U S A* **110:** E2298-E2307.

Liu Y, Gray NS (2006) Rational design of inhibitors that bind to inactive kinase conformations. *Nat Chem Biol* **2:** 358-364.

Nagar B, Bornmann WG, Pellicena P, Schindler T, Veach DR, Miller WT, Clarkson B, Kuriyan J (2002) Crystal structures of the kinase domain of c-Abl in complex with the small molecule inhibitors PD173955 and imatinib (STI-571). *Cancer Res* **62:** 4236-4243.

Parra JL, Buxade M, Proud CG (2005) Features of the catalytic domains and C termini of the MAPK signal-integrating kinases Mnk1 and Mnk2 determine their differing activities and regulatory properties. *J Biol Chem* **280:** 37623-37633.

Shao H, Shi S, Huang S, Hole AJ, Abbas AY, Baumli S, Liu X, Lam F, Foley DW, Fischer PM et al. (2013) Substituted 4-(Thiazol-5-yl)-2-(phenylamino) pyrimidines Are Highly

Active CDK9 Inhibitors: Synthesis, X-ray Crystal Structures, Structure–Activity Relationship, and Anticancer Activities. *J Med Chem* **56:** 640-659.

Sussman A, Huss K, Chio L-C, Heidler S, Shaw M, Ma D, Zhu G, Campbell RM, Park T-S, Kulanthaivel P et al. (2004) Discovery of cercosporamide, a known antifungal natural product, as a selective Pkc1 kinase inhibitor through high-throughput screening. *Eukaryot Cell* **3:** 932-943.

Teo T, Lam F, Yu M, Yang Y, K.C. Basnet S, Albrecht H, Sykes MJ, Wang S (2015a) Pharmacologic inhibition of Mnks in acute myeloid leukemia. *Mol Pharmacol* **in press**

Teo T, Yu M, Yang Y, Gillam T, Lam F, Sykes MJ, Wang S (2015b) Pharmacologic co-inhibition of Mnks and mTORC1 synergistically suppresses proliferation and perturbs cell cycle progression in blast crisis-chronic myeloid leukemia cells. *Cancer Lett* **357:** 612-623.

Tokarski JS, Newitt JA, Chang CYJ, Cheng JD, Wittekind M, Kiefer SE, Kish K, Lee FYF, Borzillerri R, Lombardo LJ et al. (2006) The structure of dasatinib (BMS-354825) bound to activated ABL kinase domain elucidates its inhibitory activity against imatinib-resistant ABL mutants. *Cancer Res* **66:** 5790-5797.

Ueda T, Sasaki M, Elia AJ, Chio IIC, Hamada K, Fukunaga R, Mak TW (2010) Combined deficiency for MAP kinase-interacting kinase 1 and 2 (Mnk1 and Mnk2) delays tumor development. *Proc Natl Acad Sci U S A* **107:** 13984-13990.

Ueda T, Watanabe-Fukunaga R, Fukuyama H, Nagata S, Fukunaga R (2004) Mnk2 and Mnk1 are essential for constitutive and inducible phosphorylation of eukaryotic initiation factor 4E but not for cell growth or development. *Mol Cell Biol* **24:** 6539-6549.

Vogtherr M, Saxena K, Hoelder S, Grimme S, Betz M, Schieborr U, Pescatore B, Robin M, Delarbre L, Langer T et al. (2006) NMR Characterization of Kinase p38 Dynamics in Free and Ligand-Bound Forms. *Angew Chem Int Ed Engl* **45:** 993-997.

Wendel HG, Silva RLA, Malina A, Mills JR, Zhu H, Ueda T, Watanabe-Fukunaga R, Fukunaga R, Teruya-Feldstein J, Pelletier J et al. (2007) Dissecting eIF4E action in tumorigenesis. *Genes Dev* **21:** 3232-3237.

Wodicka LM, Ciceri P, Davis MI, Hunt JP, Floyd M, Salerno S, Hua XH, Ford JM, Armstrong RC, Zarrinkar PP et al. (2010) Activation state-dependent binding of small molecule kinase inhibitors: structural insights from biochemistry. *Chem Biol* **17:** 1241-1249.

Yu M, Li P, K. C. Basnet S, Kumarasiri M, Diab S, Teo T, Albrecht H, Wang S (2015) Discovery of 4-(Dihydropyridinon-3-yl) amino-5-methylthieno [2, 3-d] pyrimidine Derivatives as Potent Mnk Inhibitors: Synthesis, Structure-Activity Relationship Analysis and Biological Evaluation. *Eur J Med Chem* **95:** 116-126.

Zhang J-H, Chung TD, Oldenburg KR (1999) A simple statistical parameter for use in evaluation and validation of high throughput screening assays. *J Biomol Screen* **4:** 67-73.

Zhang J, Yang PL, Gray NS (2009) Targeting cancer with small molecule kinase inhibitors. *Nat Rev Cancer* **9:** 28-39.

Molecular Pharmacology Fast Forward. Published on August 12, 2015 as DOI: 10.1124/mol.115.100131
This article has not been copyedited and formatted. The final version may differ from this version.

Footnotes

This work is supported by the Australia Government National Health and Medical Research Council [Grant 1050825], and South Australian Health and Medical Research Institute, Beat Cancer Project Principal Cancer Research Fellowship to S.W.

Molecular Pharmacology Fast Forward. Published on August 12, 2015 as DOI: 10.1124/mol.115.100131
This article has not been copyedited and formatted. The final version may differ from this version.

Figure Legends

Scheme 1. Screening cascade of Mnk inhibitor profiling. All compounds were tested with the IMAP assays at 1 and 10 µM concentrations. Compounds that showed Mnk1 or Mnk2 inhibition > 25 % at 1 µM and/or > 90 % inhibition at 10 µM were further evaluated with the ADP-Glo assay to determine their IC_{50} values. Dual and Mnk2-specific inhibitors with an IC_{50} value < 2 µM were tested for substrate competition with increasing ATP and eIF4E-derived peptide concentrations using the ADP-Glo assay. Competition effects were indicated as positive when the IC_{50} values increased by > 5 fold at elevated ATP or eIF4E peptide concentrations (see IC_{50} ratios in Table 2).

Figure 1. Optimization of the IMAP assay conditions. (A) IMAP assay principle (adapted from Molecular Devices, LLC; www.moleculardevices.com). The TAMRA labeled peptide substrate is depicted as a chain of circles with residue Ser209 marked in black. The Mnk-phosphorylated peptide will specifically bind to trivalent metal ions of the IMAP binding reagent. This will bring the TAMRA acceptor into close proximity of the Tb-donor (Tb-sensitizer complex). (B) Different quantities of recombinant Mnk1 or Mnk2 were incubated with 100 µM ATP and 5 µM TAMRA-eIF4E$_{202-214}$ to determine optimal assay conditions. Control reactions were run without the substrate. (C) Determination of TAMRA-eIF4E$_{202-214}$ substrate concentration in the IMAP assay. 100 ng of Mnk1 or 50 ng of Mnk2 were incubated with 100 µM ATP and TAMRA-eIF4E$_{202-214}$ peptide substrate at different concentrations. Reactions carried out without kinase acted as a control. (D) ATP titration for Mnks in the IMAP assay. 100 ng of Mnk1 or 50 ng of Mnk2 was incubated with 5 µM TAMRA-eIF4E$_{202-214}$ substrate at different ATP concentrations. Control reactions without Mnk1 or Mnk2 were

Molecular Pharmacology Fast Forward. Published on August 12, 2015 as DOI: 10.1124/mol.115.100131
This article has not been copyedited and formatted. The final version may differ from this version.

performed at the same time and used for background correction. (E) The control inhibitors CGP57380 and cercosporamide were tested in the IMAP assay using optimal parameters obtained from (B), (C) and (D) in 20 µL assay volume. Dose-response curves were calculated by applying a 4-parameter logistic non-linear regression model.

Figure 2. Compound profiling with the IMAP assay. A collection of 66 compounds was analyzed for their inhibitory activities against Mnk1 (A) and Mnk2 (B) using the IMAP assays. The compound concentrations used were 1 µM and 10 µM in duplicate and residual kinase activities were calculated as percentages relative to negative and positive controls (n = 4). The data are represented as means of 2 replicates. The lines indicate the cut-off values of 75% and 10% residual kinase activity at 1 µM and 10 µM inhibitor concentrations, respectively. In order to assess assay robustness, duplicate values were plotted against each other and linear regression was carried out (C and D). The calculated R^2 values were close to 0.9, indicating a good correlation between two duplicates and validating the sufficient robustness of the assays. The data were collected from 14 independent experiments for both Mnk1 and Mnk2. All experiments included 4 positive and 4 negative controls which were used to calculate the Z'-factors, which were > 0.5 in all cases, indicating the sufficient robustness of the assays.

Figure 3. ADP-Glo assay validation with Mnks. (A) ADP-Glo assay principle (adapted from Promega Corporation). ATP is converted into ADP when exposed to Mnk and $eIF4E_{202-214}$. The ADP-Glo reagent is used to stop the reaction and enzymatically remove remaining ATP. Subsequently, the kinase detection reagent is applied to convert ADP into ATP, which then will drive a luciferase reaction turning over beetle luciferin to generate light. (B) Different

amounts of Mnk1 or Mnk2 as indicated in Figure 3B were used in kinase reactions with fixed substrate concentrations of 100 µM ATP and 100 µM of eIF4E$_{202-214}$ peptide substrate. The obtained luminescence signals were compared to control reactions without the peptide substrate. The S/B ratios with 100 ng Mnk1 and 30 ng Mnk2 were 6.3 and 3.4, respectively. For all further experiments 100 ng Mnk1 and 30 ng Mnk2 were applied. (C) The V_{max} and K_m values were determined for the eIF4E$_{202-214}$ peptide substrate. The ATP concentration was adjusted to 2 mM and 100 ng Mnk1 or 30 ng Mnk2 were used in all reactions which were tested at different eIF4E$_{202-214}$ peptide substrate concentrations. All data were baseline corrected with signals obtained from kinase control reactions (without peptide substrate) prior to curve fitting using the Michaelis-Menten model. (D) The determination of V_{max} and K_m values for ATP was carried out under identical conditions as described for panel C, with the difference that the eIF4E$_{202-214}$ peptide substrate concentration was fixed at 1.2 mM while different ATP concentrations were used. Control reactions without kinase were performed at the same time and used for background correction prior to fitting with the Michaelis-Menten model. (E) The control inhibitors CGP57380 and cercosporamide were used for final validation of the ADP-Glo assays using above parameters in a final assay volume of 15 µL. The ATP and eIF4E$_{202-214}$ peptide substrate concentrations were adjusted to 0.5 × K_m and K_m for Mnk1 and Mnk2, respectively. Dose-response curves were calculated by iterative fitting to a 4-parameter logistic non-linear regression model. For all further experiments 0.5 × K_m values for ATP and peptide were used for Mnk1 and K_m values were used for Mnk2. (F) Dose response experiments were used to calculate IC_{50} values, which lead to the identification of 13 non-specific Mnk1/2 inhibitors and 7 Mnk2 specific inhibitors (for more details see Table 2). The latter were considered absolute Mnk2 selective inhibitors with the calculated ratio of $IC_{50Mnk1}/IC_{50Mnk2} > 10$ (note that for compounds where no IC_{50} fit could be achieved, the value was set to = 15 µM). No Mnk1 specific inhibitors were found.

Molecular Pharmacology Fast Forward. Published on August 12, 2015 as DOI: 10.1124/mol.115.100131
This article has not been copyedited and formatted. The final version may differ from this version.

Figure 4. Competition of inhibitor activity with increased ATP and eIF4E peptide substrate concentration on Mnk2. 30 ng of Mnk2 was mixed with 10 different concentrations of Mnk inhibitors and the ADP-Glo assay was performed in the presence of increasing concentrations of ATP (A, B and C) and with increasing concentrations of $eIF4E_{202-214}$ peptide substrate (D, E and F). All experiments were run in duplicates and the values from individual samples were analyzed using the Prism 6 Graphpad software. The three compounds were selected as examples for the different inhibition modes (MNKI-6: -/-; MNKI-4-61: +/-; MNKI-5-17: +/+). (G) Compound structures.

Figure 5. The same compounds as shown in Figure 4 were used to determine the apparent K_m and V_{max} values at different compound concentrations. The Michaelis-Menten saturation curves are given for a range of ATP (panels A-C) and a range of $eIF4E_{202-214}$ concentrations (panels D-F). Selected compounds were used at the concentrations as indicated in the figure. The calculated kinetic parameters are given beneath the shown graphs.

Figure 6. Cytotoxic effects correlate with Mnk enzyme inhibition. MV4-11 cells were exposed to compounds for 72 h. The resazurin assay was used to test cell viability in dose response experiments and GI_{50} values were calculated. Compounds with activities against CDK2A or CDK9T1 (K_i □ 15 μM) were excluded. (A) The IC_{50} values for Mnk1 were plotted against the GI_{50} values. Compounds with IC_{50} values □ 10 μM against Mnk1 were excluded and the data are given for 14 compounds. (B) A similar plot was generated with the Mnk2 data with 17 compounds in total. The trend lines are shown and the Pearson

correlations were determined for Mnk1 (r = 0.4006; n = 14; one tailed p = 0.078) and Mnk2 (r = 0.7276; n = 17; one tailed p = 0.0005). Western blot analysis was conducted with MV4-11 cells after 1 hour exposure to MNKI-7 (C) or MNKI-19 (D) at the concentrations indicated.

Figure 7. (A) Structures of some selected compounds. Very subtle changes of MNKI-5 induce a switch from mode -/- to mode +/- (MNKI-15) or dramatically reduce potency by more than factor 10 against Mnk1 (MNKI-37). The efficacy of MNKI-37 against Mnk1 was significantly improved through modification of the acetamide group as shown for MNKI-83 (B) Hypothetical working model for compound binding at reactive site. The Mnks switch from the inactive DFD-out form (I) to the active DFD-in form (II) upon phosphorylation of the activation segment and subsequently bind the ATP substrate. (III) The cartoon depicts MNKI-15 as a Type II kinase inhibitor binding partly inside and partly adjacent to the ATP binding pocket. The black diamond represents the common core scaffold between MNKI-15 and -5 which occupies the postulated allosteric binding site. (IV) Hypothetical binding modalities of MNKI-5: The larger side chain is forced through steric hindering (dashed structure) to adopt an alternative conformation with non-ATP-competitive binding mode.

Molecular Pharmacology Fast Forward. Published on August 12, 2015 as DOI: 10.1124/mol.115.100131
This article has not been copyedited and formatted. The final version may differ from this version.

Table 1. Kinetic constants for Mnks.

Kinase	Mnk1		Mnk2	
Substrate	ATP	$eIF4E_{202-214}$	ATP	$eIF4E_{202-214}$
K_m (μM)	2094	1272	215.8	608.5
V_{max} (nmol/min)	0.18523	0.21718	0.03225	0.05537
Specific activity (nmol/min/mg)	1852	2172	1075	1846
Compound	CGP57380	Cercosp.	CGP57380	Cercosp.
K_i value (μM)	1.010	0.507	0.877	0.079

Molecular Pharmacology Fast Forward. Published on August 12, 2015 as DOI: 10.1124/mol.115.100131
This article has not been copyedited and formatted. The final version may differ from this version.

Table 2. Summary of Mnk inhibitory activity, binding mode and cellular anti-proliferative activity of compounds.

Compound		IC_{50} (nM)		IC_{50} ratio						MV4-11 cells[3]	
				Mnk1			Mnk2				
Code	Series	Mnk1	Mnk2	ATP $(\frac{6\ mM}{0.15\ mM})$	eIF4E $(\frac{3\ mM}{0.15\ mM})$	Mode	ATP $(\frac{2\ mM}{0.05\ mM})$	eIF4E $(\frac{3\ mM}{0.15\ mM})$	Mode	GI_{50} (μM)	SD
MNKI-6	1	47	20	2.2	1.9	-/-	1.9	1.1	-/-	0.58	0.02
MNKI-7	1	83	44	1.5	1.2	-/-	1.0	1.0	-/-	0.83	0.03
MNKI-5	1	147	50	1.8	1.0	-/-	1.1	0.9	-/-	27.77	3.96
MNKI-57	1	159	36	2.4	1.7	-/-	4.1	1.5	-/-	6.00	0.79
MNKI-8	1	164	52	1.8	1.5	-/-	4.1	0.9	-/-	1.15	0.57
MNKI-19	1	279	136	1.7	1.0	-/-	1.6	1.3	-/-	7.30	0.75
MNKI-83	1	480	328	2.3	2.8	-/-	2.4	0.8	-/-	15.30	2.62
MNKI-67[2]	1	1400	36	2.2	1.4	-/-	1.5	1.0	-/-	8.84	1.58
MNKI-37	1	1530	219	1.9	1.1	-/-	1.1	0.8	-/-	6.08	1.99
MNKI-15	1	2850	328	14.5	1.5	+/-	6.4	2.0	+/-	78.26	2.34
MNKI-2-22	1	3090	480	7.2	1.9	+/-	3.5	7.6	-/+	59.58	3.48
MNKI-2-30	1	3225	1810	10.2	1.4	+/-	15.2	1.2	+/-	88.99	4.11
MNKI-2-25	1	3495	678	50.2	1.8	+/-	37.8	0.9	+/-	13.96	2.21
MNKI-28[2]	1	7230	704	NT	NT		11.6	1.1	+/-	15.18	1.91
MNKI-85[2]	1	□ 10000	62	NT	NT		15.2	1.2	+/-	7.44	0.77
MNKI-4[2]	1	> 10000	452	NT	NT		12.9	1.0	+/-	8.88	0.54
MNKI-12[2]	1	> 10000	1000	NT	NT		18.6	2.3	+/-	89.39	9.58
MNKI-7-50	3	4800	1540	NT	NT		35.7	1.4	+/-	NA[1]	
MNKI-5-17[2]	2	> 10000	618	NT	NT		76.6	37.7	+/+	NA[1]	
MNKI-4-61[2]	2	> 10000	1230	NT	NT		16.4	1.3	+/-	NA[1]	

Molecular Pharmacology Fast Forward. Published on August 12, 2015 as DOI: 10.1124/mol.115.100131
This article has not been copyedited and formatted. The final version may differ from this version.

Series = compound series; eIF4E = $eIF4E_{202-214}$; Mode: ATP/$eIF4E_{202-214}$ competition; [1)]*K*i value < 15 µM on CDK2A or CDK9T1; [2)]mono-specific Mnk2 inhibitor; NA, not active; NT, not tested; [3)] by 72 h resazurin assay; data shown are the mean values derived from at least two replicates.

Molecular Pharmacology Fast Forward. Published on August 12, 2015 as DOI: 10.1124/mol.115.100131
This article has not been copyedited and formatted. The final version may differ from this version.

Figure 1.

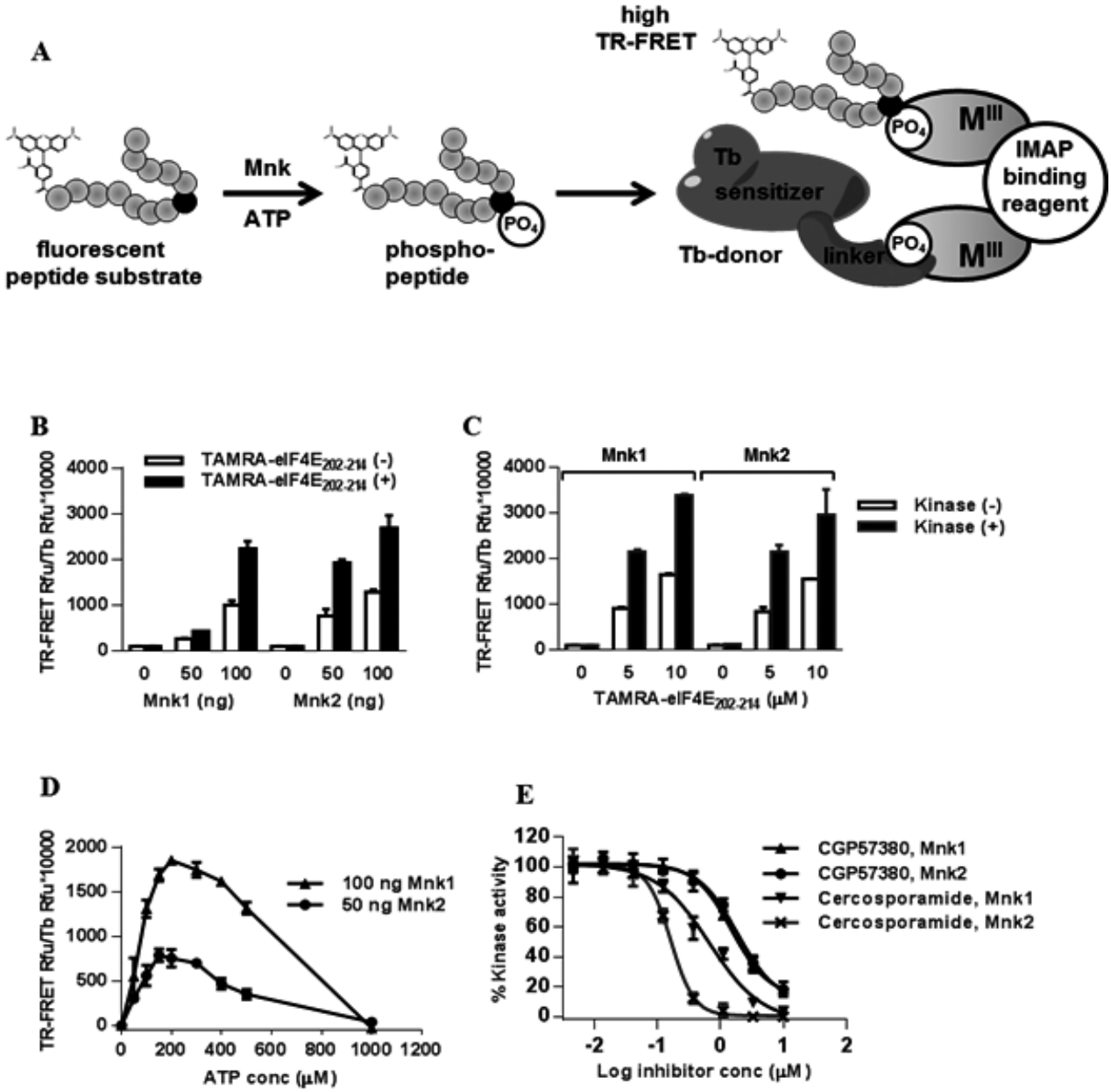

Molecular Pharmacology Fast Forward. Published on August 12, 2015 as DOI: 10.1124/mol.115.100131
This article has not been copyedited and formatted. The final version may differ from this version.

Figure 2.

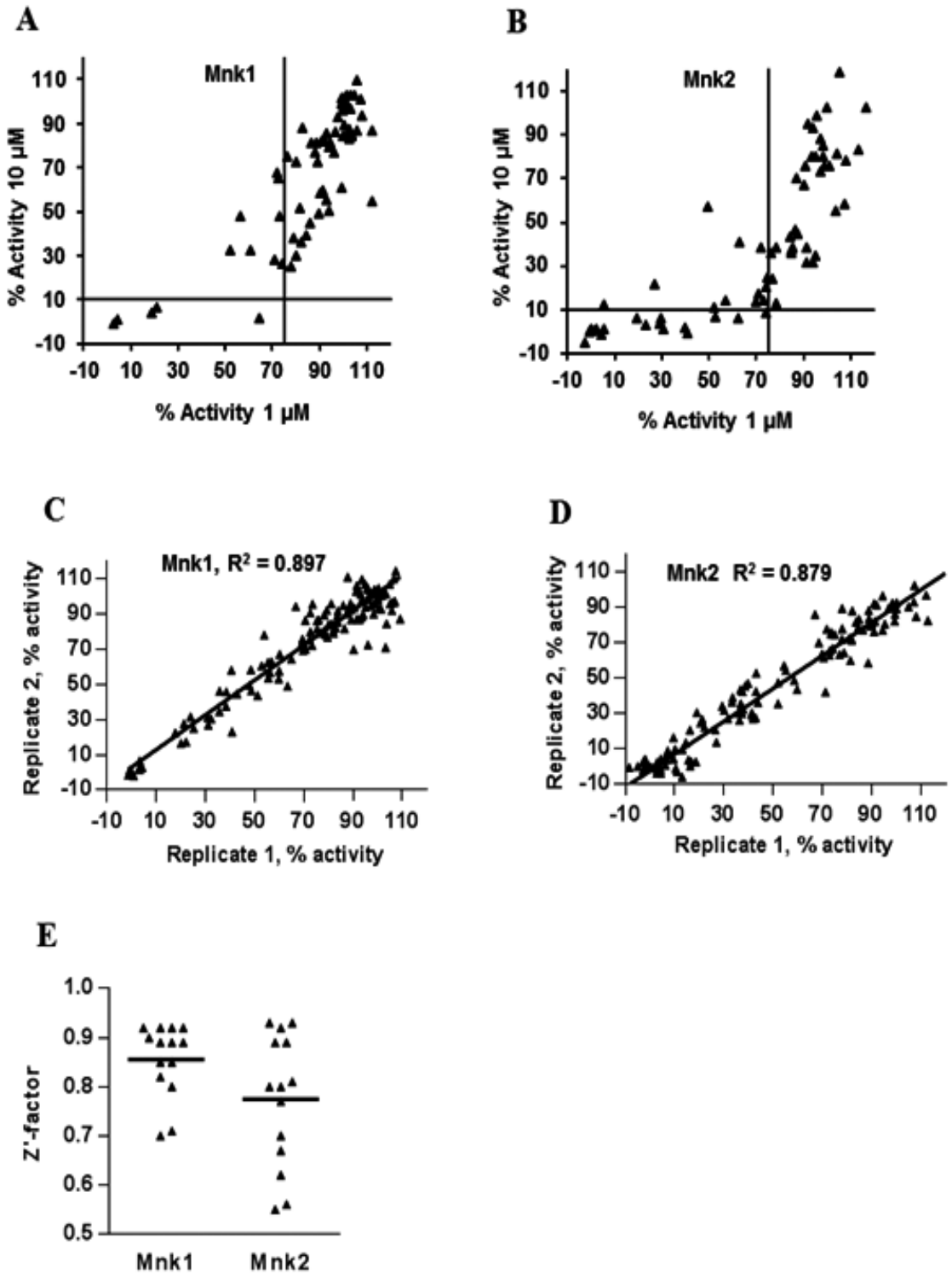

Molecular Pharmacology Fast Forward. Published on August 12, 2015 as DOI: 10.1124/mol.115.100131
This article has not been copyedited and formatted. The final version may differ from this version.

Figure 3.

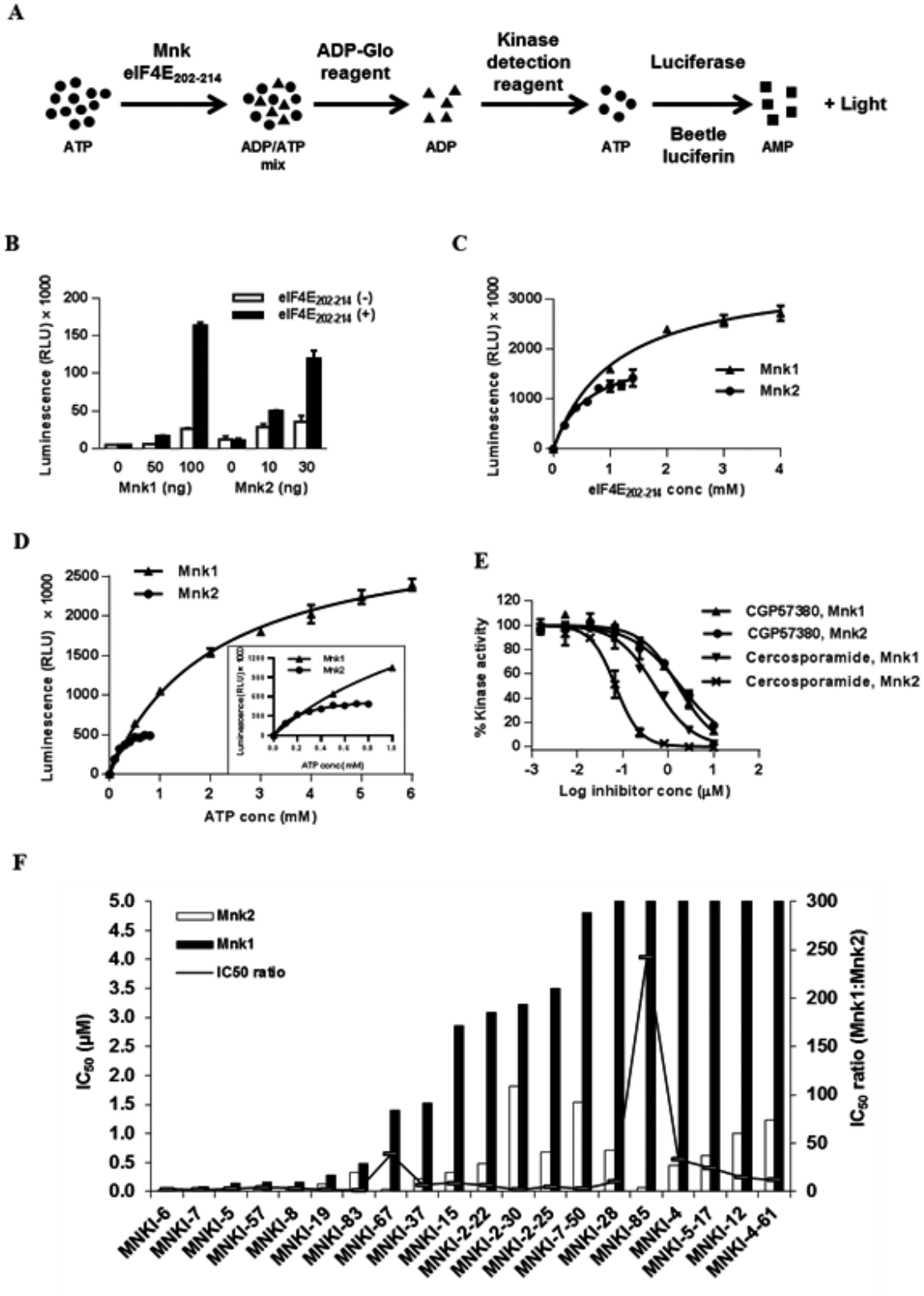

Molecular Pharmacology Fast Forward. Published on August 12, 2015 as DOI: 10.1124/mol.115.100131
This article has not been copyedited and formatted. The final version may differ from this version.

Figure 4.

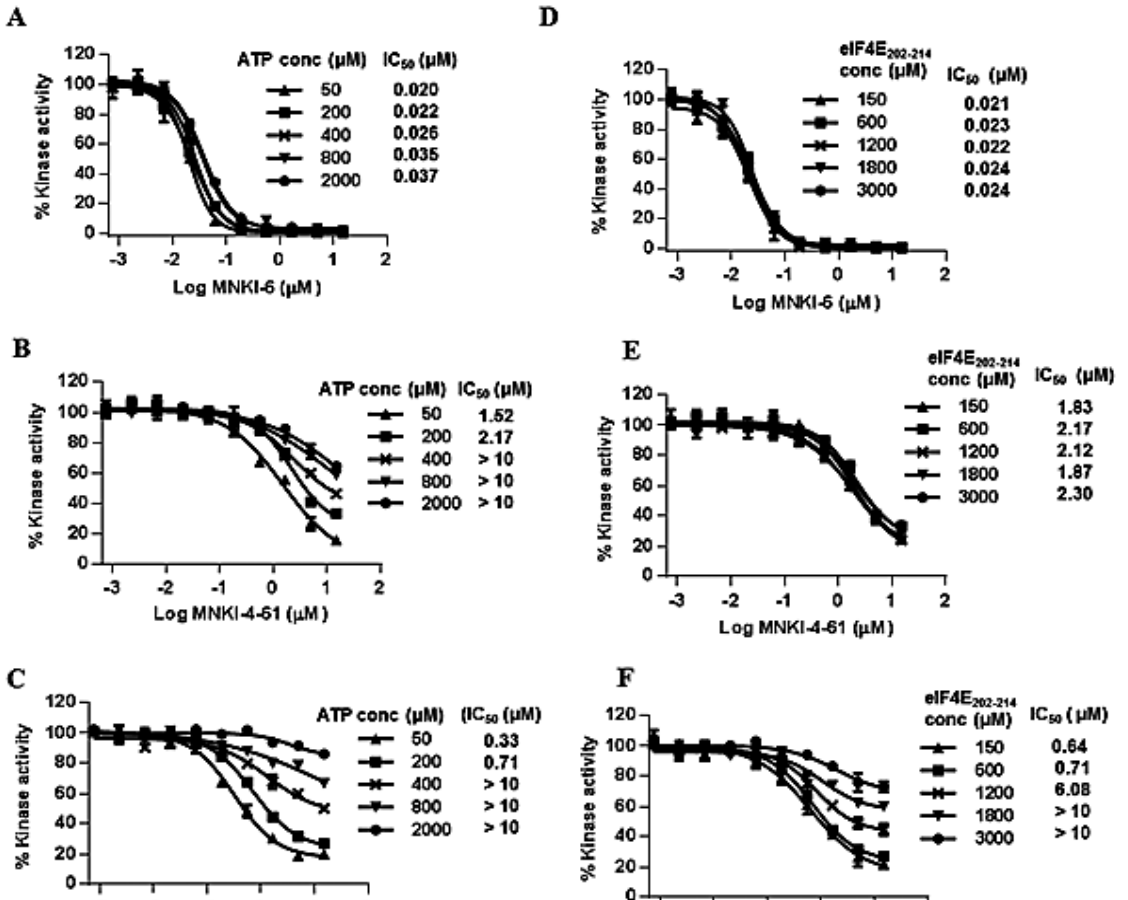

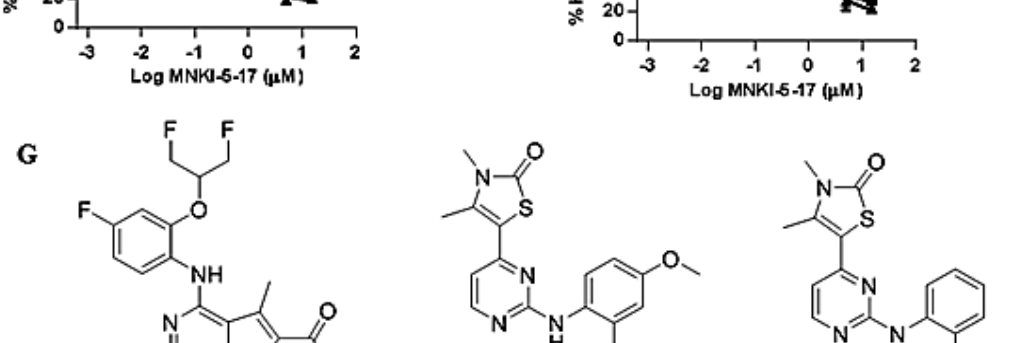

Molecular Pharmacology Fast Forward. Published on August 12, 2015 as DOI: 10.1124/mol.115.100131
This article has not been copyedited and formatted. The final version may differ from this version.

Figure 5.

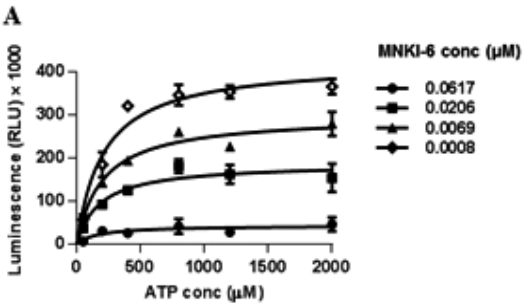

MNKI-6 (μM)	0.0617	0.0206	0.0069	0.0008
K_m	209.2	217.3	221.0	220.5
V_{max}	48324	200533	308953	424584

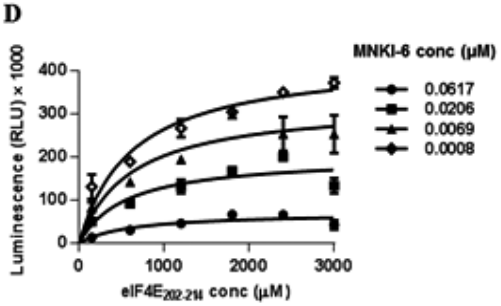

MNKI-6 (μM)	0.0617	0.0206	0.0069	0.0008
K_m	610.6	559.6	608.2	621.7
V_{max}	71369	202138	336471	429222

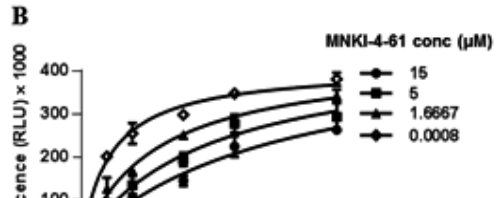

MNKI-4-61 (μM)	15	5	1.6667	0.0008
K_m	1305	972.7	613.6	218.9
V_{max}	446000	438730	437260	404199

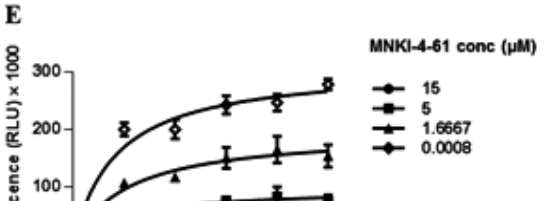

MNKI-4-61 (μM)	15	5	1.6667	0.0008
K_m	605.4	587.8	623.0	600.6
V_{max}	47561	97892	196820	621999

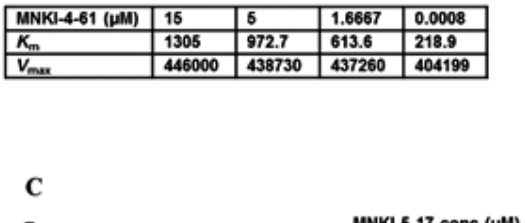

MNKI-5-17 (μM)	15	5	1.6667	0.0008
K_m	1313	740.1	440.5	220.2
V_{max}	490078	481574	453057	425231

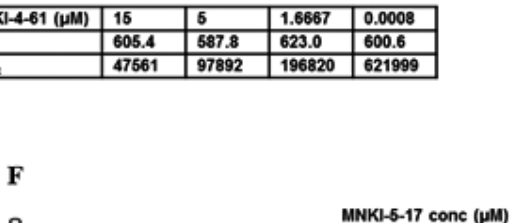

MNKI-5-17 (μM)	15	5	1.6667	0.0008
K_m	2442	1691	1088	602.4
V_{max}	441137	428639	409377	460130

Molecular Pharmacology Fast Forward. Published on August 12, 2015 as DOI: 10.1124/mol.115.100131
This article has not been copyedited and formatted. The final version may differ from this version.

Figure 6.

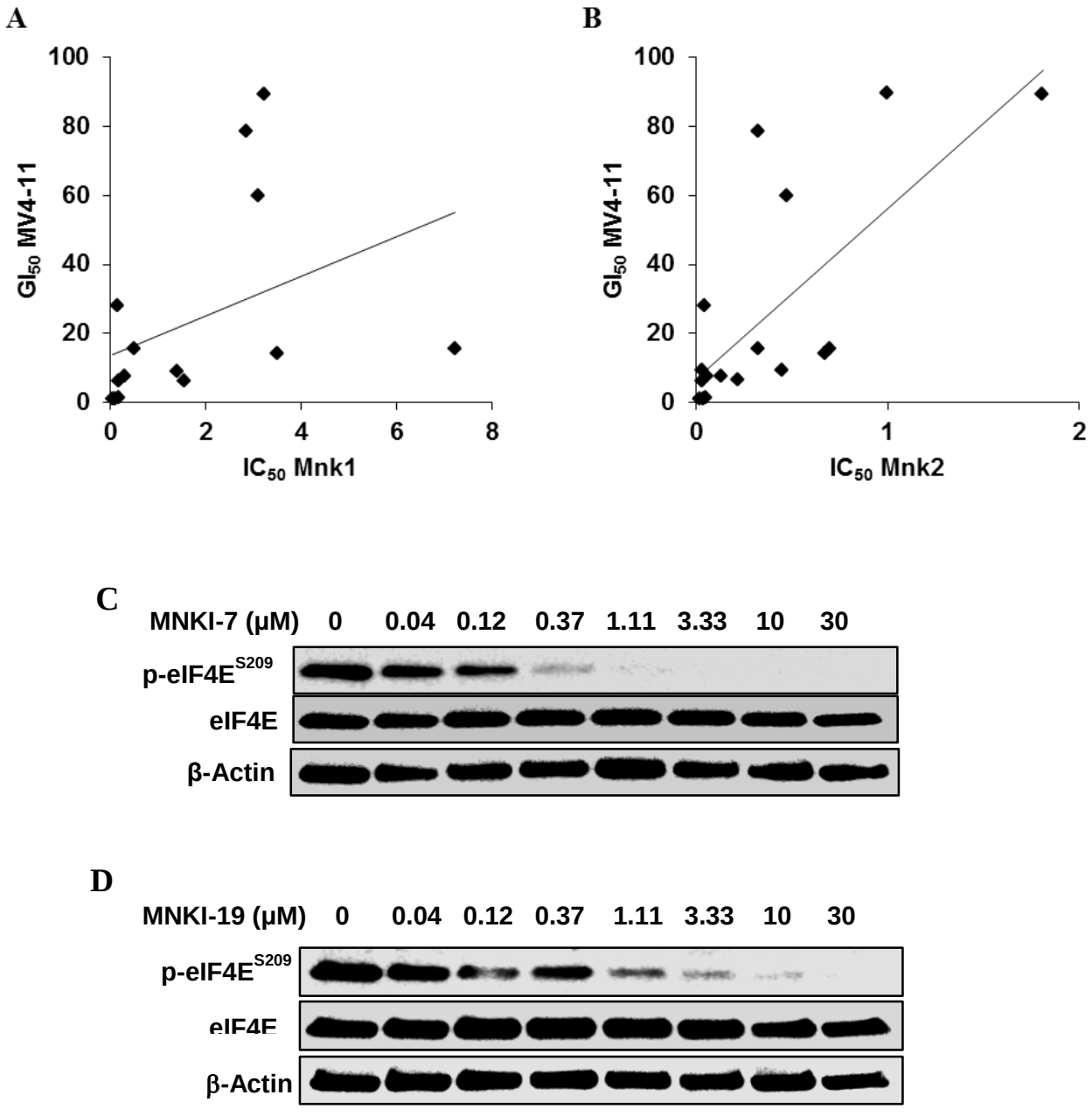

Molecular Pharmacology Fast Forward. Published on August 12, 2015 as DOI: 10.1124/mol.115.100131
This article has not been copyedited and formatted. The final version may differ from this version.

Figure 7.